Description of the giant monopole resonance in the even-A $^{112-124}$Sn isotopes within a microscopic model including quasiparticle-phonon coupling

V. Tselyaev,[1,2] J. Speth,[1] S. Krewald,[1] E. Litvinova,[3,4,5] S. Kamerdzhiev,[1,5] N. Lyutorovich,[1,2]
A. Avdeenkov,[1,6] and F. Grümmer[1]

[1]*Institut für Kernphysik, Forschungszentrum Jülich, D-52425 Jülich, Germany*
[2]*Nuclear Physics Department, V. A. Fock Institute of Physics, St. Petersburg State University, RU-198504 St. Petersburg, Russia*
[3]*Gesellschaft für Schwerionenforschung mbH, D-64291 Darmstadt, Germany*
[4]*Frankfurt Institute for Advanced Studies, Universität Frankfurt, D-60438 Frankfurt am Main, Germany*
[5]*Institute of Physics and Power Engineering, RU-249033 Obninsk, Russia*
[6]*Skobeltsyn Institute of Nuclear Physics, Moscow State University, RU-119991 Moscow, Russia*

(Received 6 October 2008; published 10 March 2009)

We have calculated the strength distributions of the isoscalar giant monopole resonance (ISGMR) in the even-A tin isotopes ($A = 112$–124) that were recently measured in inelastic α scattering. The calculations were performed within two microscopic models: the quasiparticle random phase approximation (QRPA) and the quasiparticle time blocking approximation (QTBA), which is an extension of the QRPA including quasiparticle-phonon coupling. We used a self-consistent calculational scheme based on the Hartree-Fock+Bardeen-Cooper-Schrieffer approximation. Within the RPA the self-consistency is full. The single-particle continuum is also exactly included at the RPA level. The self-consistent mean field and the effective interaction are derived from the Skyrme energy functional. In the calculations, two Skyrme force parametrizations were used: T5 with a comparatively low value of the incompressibility modulus of infinite nuclear matter ($K_\infty = 202$ MeV) and T6 with $K_\infty = 236$ MeV. The T5 parametrization gives theoretical results for tin isotopes in good agreement with the experimental data including the resonance widths. The results of the ISGMR calculations in ^{90}Zr, ^{144}Sm, and ^{208}Pb performed with these Skyrme forces are discussed and compared with the experiment.

DOI: 10.1103/PhysRevC.79.034309 PACS number(s): 21.60.−n, 24.30.Cz, 25.55.Ci, 27.60.+j

I. INTRODUCTION

The investigation of the isoscalar giant monopole resonance (ISGMR), the so-called breathing mode, is one of the fundamental problems of nuclear physics. The energy of the ISGMR enables one to determine parameters characterizing the incompressibility of infinite nuclear matter (INM), in particular, the value of the incompressibility modulus K_∞, which in turn is a universal characteristic of the effective nuclear forces. These collective resonances can be studied experimentally in inelastic α scattering at small angles (see, e.g., Ref. [1] and references therein). Theoretical investigations of these states are based mainly on (i) the self-consistent microscopic approaches (see, e.g., Refs. [2–12]), including scaling and constrained Hartree-Fock (HF) methods and the random phase approximation (RPA), and (ii) the Landau-Migdal approach, which starts with a phenomenological single-particle basis and with the independently parametrized particle-hole zero-range interaction (see, e.g., Refs. [13–15] and references therein). It is important to note that the incompressibility modulus K_∞ cannot be measured directly but it can be deduced theoretically by comparing the experimental energies of the ISGMR with the corresponding calculated values. The most widely used approach is based on the self-consistent HF or RPA calculations of the mean energies of the ISGMR using effective Skyrme or Gogny forces. Because K_∞ can be calculated from the known parameters of the given force, its value is estimated as the one corresponding to the force that gives the best description of the experimental data. The nonrelativistic estimates obtained in such a way lead to the value $K_\infty = 210 \pm 30$ MeV (see, e.g., Refs. [2,4–10]), though the recent results testify to the upper limit of this estimate (see Refs. [11,12]). In the Landau-Migdal approach one obtains K_∞ from the scalar-isoscalar Landau-Migdal parameter f_0. Here K_∞ was always of the order of 240 MeV [13].

Note that within the relativistic mean-field (RMF) theory the INM incompressibility is usually restricted to the interval $K_\infty = 260 \pm 10$ MeV (see, e.g., Ref. [16]), which is considerably higher than the nonrelativistic limits. However, recently a zero-range (point-coupling) representation of the effective nuclear interactions in the RMF framework was found to lead to the reduction of K_∞ up to the value of 230 MeV [17].

In the present paper we investigate theoretically the experimental data [18] on the strength distributions of the ISGMR in the even-A tin isotopes ($A = 112$–124) that were recently measured with inelastic scattering of α particles at RCNP (Osaka University). This is the main goal of our work. The calculations are performed within the framework of the recently developed microscopic model that takes into account the effects of the quasiparticle-phonon coupling (QPC) in addition to the usual correlations included in the conventional RPA.

The paper is organized as follows. In Sec. II the model is described, with particular attention paid to dynamical pairing effects, which are important for solving the problem of the 0^+ spurious state in the ISGMR calculations in open-shell nuclei. In Sec. III we describe the details of our calculational scheme and present and discuss the results. Conclusions are drawn in the last section. Appendices contain auxiliary formulas.

II. THE MODEL

A. General scheme

Two microscopic models were used in our calculations. The first is the well-known quasiparticle RPA (QRPA). The basic ingredients of this approximation are the nuclear mean field (including the pairing field operator) and the residual particle-hole (ph) interaction. In the self-consistent QRPA these ingredients are related to each other by the consistency condition. The nuclear excitations are treated as superpositions of the two-quasiparticle (2q) configurations. This model is applicable to a wide range of nuclei including open-shell ones as the pairing correlations of nucleons are taken into account. The QRPA reproduces well the centroid energies and total strengths of giant multipole resonances but not their widths. To reproduce the total widths of the resonances it is necessary to enlarge the configuration space by adding 4q configurations [i.e., to extend the (Q)RPA]. The most successful approaches in this direction are the models that take into account the QPC in addition to the correlations included in the (Q)RPA (see, e.g., Refs. [15,19,20] and references therein).

In the present investigation the QPC contributions are included within the framework of the recently developed quasiparticle time blocking approximation (QTBA), which is an extension of the QRPA in this sense. On the other hand, since in the QTBA the pairing correlations are also included, this model is a generalization of the method of chronological decoupling of diagrams [21], which is a base of the extended theory of finite Fermi systems [15]. Details of the QTBA model are described in Refs. [22,23]. The basic equation of our approach (both in the QRPA and in the QTBA) is the equation for the effective response function $R^{\rm eff}(\omega)$. In the shorthand notation following that of Ref. [23] it reads

$$R^{\rm eff}(\omega) = A(\omega) - A(\omega)\,\mathcal{F}R^{\rm eff}(\omega), \tag{1}$$

where $A(\omega)$ is a correlated propagator and $\mathcal{F}$ is an amplitude of the effective residual interaction. In the case of the QRPA, $A(\omega)$ reduces to the uncorrelated 2q propagator $\tilde{A}(\omega)$. In the general case including pairing correlations, the amplitude $\mathcal{F}$ can be represented as a sum of two terms,

$$\mathcal{F} = \mathcal{F}^{\rm (ph)} + \mathcal{F}^{\rm (pp)}, \tag{2}$$

where the amplitude $\mathcal{F}^{\rm (ph)}$ represents interaction in the ph channel and $\mathcal{F}^{\rm (pp)}$ includes contributions of the interaction both in the particle-particle (pp) and in the hole-hole (hh) channels. (In the following for brevity we will use the unified term pp channel, implying also the hh-channel contributions.)

Let us emphasize that the general formulas of the QTBA derived in Ref. [22] are valid both in the self-consistent and in the non-self-consistent approaches. In the present paper, we use a self-consistent calculational scheme based on the HF and Bardeen-Cooper-Schrieffer (BCS) approximations (henceforth referred to as the HF+BCS approximation). The self-consistent mean field and the effective residual interaction are derived from the Skyrme energy functional by means of the known variational equations. In the calculations, the T5 and T6 Skyrme forces (see Ref. [24]) are used.

An important property of these parametrizations is that they produce the nucleon effective mass m^* equal to the bare nucleon mass m. This is a consequence of the fact that the T5 and T6 Skyrme-force parameters are constrained by the relations (see Ref. [25])

$$t_2 = -\frac{1}{3}\,t_1\,(5+4x_1), \quad x_2 = -\frac{4+5\,x_1}{5+4\,x_1}. \tag{3}$$

In this case the contribution of the velocity-dependent terms (except for the spin-orbital ones) to the energy functional and the mean field reduces to the derivatives of the nucleon density (i.e., to the simple surface terms). As a consequence, the contribution of these terms into the effective interaction derived from such an energy functional also has a very simple form. To see this, consider the energy density $\mathcal{H}$ of the Skyrme energy functional $\mathcal{E}$ defined as

$$\mathcal{E} = \int d\boldsymbol{r}\,\mathcal{H}(\boldsymbol{r}). \tag{4}$$

In the sufficiently general case it is given, for example, in Ref. [24]. However, if Eq. (3) holds, the energy density acquires the form

$$\begin{aligned}\mathcal{H} = {}& \frac{\hbar^2}{2m}(\tau_n+\tau_p) + \frac{1}{2}\,t_0\left[\left(1+\frac{1}{2}\,x_0\right)\rho^2 - \left(x_0+\frac{1}{2}\right)\right.\\ & \left.\times\left(\rho_n^2+\rho_p^2\right)\right] + \frac{1}{16}\,t_1\left\{3\left(1+\frac{1}{2}\,x_1\right)\right.\\ & \times(\nabla\rho)^2 - 3\left(x_1+\frac{1}{2}\right)\left[(\nabla\rho_n)^2+(\nabla\rho_p)^2\right]\\ & \left.- x_1\boldsymbol{J}^2 + \boldsymbol{J}_n^2 + \boldsymbol{J}_p^2\right\} - \frac{1}{16}\,t_2\left\{\left(1+\frac{1}{2}\,x_2\right)(\nabla\rho)^2\right.\\ & + \left(x_2+\frac{1}{2}\right)\left[(\nabla\rho_n)^2+(\nabla\rho_p)^2\right] + x_2\boldsymbol{J}^2 + \boldsymbol{J}_n^2 + \boldsymbol{J}_p^2\Big\}\\ & + \frac{1}{12}\,t_3\left[\left(1+\frac{1}{2}\,x_3\right)\rho^2 - \left(x_3+\frac{1}{2}\right)\left(\rho_n^2+\rho_p^2\right)\right]\rho^\alpha\\ & + \frac{1}{2}\,W_0\left(\boldsymbol{J}\cdot\nabla\rho + \boldsymbol{J}_n\cdot\nabla\rho_n + \boldsymbol{J}_p\cdot\nabla\rho_p\right)\\ & + \mathcal{H}_{\rm Coul} + \mathcal{H}_{\rm pair},\end{aligned} \tag{5}$$

where $\mathcal{H}_{\rm Coul}$ is the Coulomb energy density including the exchange part in the Slater approximation, that is,

$$\mathcal{H}_{\rm Coul}(\boldsymbol{r}) = \frac{e^2}{2}\int d\boldsymbol{r}'\,\frac{\rho_p(\boldsymbol{r})\,\rho_p(\boldsymbol{r}')}{|\boldsymbol{r}-\boldsymbol{r}'|} - e^2\,\frac{3}{4}\left(\frac{3}{\pi}\right)^{1/3}\rho_p^{4/3}(\boldsymbol{r}), \tag{6}$$

and $\mathcal{H}_{\rm pair}$ is the density of the pairing energy. In the applications of the models based on the Skyrme energy functionals it is frequently taken in the simplest form

$$\mathcal{H}_{\rm pair} = \tfrac{1}{4}\,V_0\,(\varkappa_n^*\varkappa_n + \varkappa_p^*\varkappa_p), \tag{7}$$

which was also used in our calculations. In Eqs. (5)–(7), ρ_q, τ_q, and $\boldsymbol{J}_q$ are the normal densities and $\varkappa_q$ is the anomalous local density of the nucleons of the type $q = n, p$ (neutrons or protons); $\rho = \rho_n + \rho_p$ and $\boldsymbol{J} = \boldsymbol{J}_n + \boldsymbol{J}_p$. In particular, ρ_q is the local particle density, τ_q is the kinetic-energy density, and $\boldsymbol{J}_q$ is the spin density. They are defined in the usual way (see, e.g., Ref. [26]). In the case of the spherically symmetric

nucleus and within the HF+BCS approximation they have the form

$$\rho_q(r) = \sum_{(1)} \delta_{q_1,q} \frac{2j_1+1}{4\pi} v^2_{(1)} R^2_{(1)}(r), \tag{8}$$

$$\tau_q(r) = \sum_{(1)} \delta_{q_1,q} \frac{2j_1+1}{4\pi} v^2_{(1)} \left[(R'_{(1)}(r))^2 + \frac{l_1(l_1+1)}{r^2} R^2_{(1)}(r) \right], \tag{9}$$

$$\boldsymbol{J}_q(r) = \frac{\boldsymbol{r}}{r^2} \sum_{(1)} \delta_{q_1,q} \frac{2j_1+1}{4\pi} v^2_{(1)} \left[j_1(j_1+1) - l_1(l_1+1) - \frac{3}{4} \right] R^2_{(1)}(r), \tag{10}$$

$$\varkappa_q(r) = \sum_{(1)} \delta_{q_1,q} \frac{2j_1+1}{4\pi} u_{(1)} v_{(1)} R^2_{(1)}(r). \tag{11}$$

Here and in the following we use the notation of Refs. [22,23] for the single-quasiparticle basis functions in the doubled space $\tilde{\psi}_1$, which are labeled by the composite indices $1 = \{[1], m_1\}$, where $[1] = \{(1), \eta_1\}$, $(1) = \{q_1, n_1, l_1, j_1\}$, and $\eta_1 = \pm 1$ is the sign of the quasiparticle energy $E_1 = \eta_1 E_{(1)}$. That is, the symbol "(1)" stands for the set of the single-particle quantum numbers except for the projection of the total angular momentum m_1, $R_{(1)}(r)$ is the radial part of the single-particle wave function, $v^2_{(1)}$ is the occupation probability, and $u_{(1)} = \sqrt{1 - v^2_{(1)}}$.

Equations (4) and (5) result in the following equality:

$$\frac{\delta \mathcal{E}}{\delta \tau_q(\boldsymbol{r})} = \frac{\hbar^2}{2m} = \text{constant}. \tag{12}$$

In particular, this means that the equations of motion derived from such an energy functional $\mathcal{E}$ contain the nucleon effective mass $m^*_q(r) = m$. The spin-scalar part of the effective residual interaction in the ph channel corresponding to $\mathcal{E}$ is determined by the relation

$$\mathcal{F}^{(\mathrm{ph})}_{0,qq'}(\boldsymbol{r}, \boldsymbol{r}') = \frac{\delta^2 \mathcal{E}}{\delta \rho_q(\boldsymbol{r})\, \delta \rho_{q'}(\boldsymbol{r}')}. \tag{13}$$

This ansatz completely includes velocity-dependent contributions because of Eq. (12). The explicit form of this part of the interaction in the case of the functional [Eq. (5)] is shown in Appendix A.

As can be seen from Eqs. (A1) and (A2), the density-dependence power of the effective nuclear forces is set by the parameter α of the Skyrme energy functional. There exists the following simple relationship between this parameter and the INM incompressibility modulus K_∞:

$$K_\infty = K^{(0)}_\infty + K^{(1)}_\infty \alpha, \tag{14}$$

where

$$K^{(0)}_\infty = \left[1 + 4 \left(\frac{m}{m^*} - 1 \right) \right] \frac{3}{5} \frac{\hbar^2 k_F^2}{2m} + 9 \frac{B}{A}, \tag{15}$$

$$K^{(1)}_\infty = \left[1 - 2 \left(\frac{m}{m^*} - 1 \right) \right] \frac{9}{5} \frac{\hbar^2 k_F^2}{2m} + 9 \frac{B}{A}, \tag{16}$$

with k_F and B/A being the Fermi momentum and the binding energy per nucleon in nuclear matter, respectively. Putting $k_F = 1.35$ fm^{-1}, $B/A = 16$ MeV, and $m^* = m$ one gets (see Ref. [4])

$$K_\infty = 167 + 212\,\alpha \text{ (MeV)}. \tag{17}$$

Thus, for the typical values of α we have $K_\infty = 202$ MeV for $\alpha = 1/6$ and $K_\infty = 237$ MeV for $\alpha = 1/3$.

Let us note that in addition to the simplicity of the formulas for the residual interaction there are physical reasons to use the effective forces with $m^* = m$. It is known that for heavy and medium mass nuclei the single-particle spectra obtained in the HF calculations with such forces better reproduce the experimental energies as compared with the case of the forces with $m^*/m \sim 0.7$. As a rule, this results in better description of the excitations of the even-mass nuclei in the RPA and QRPA. The same is true for the QTBA if the subtraction procedure (see Eq. (21) in the next section and Refs. [22,23]) is used.

The spin-vector components of the effective interaction are not determined uniquely from Eq. (5), which is valid only for the spin-saturated nuclei. However, these components do not enter equations for the 0^+ excitations. The spin-orbital components of the residual interaction in the general case lead to considerable complication of the formulas. But for the monopole excitations the situation is simplified. In our calculations the spin-orbital components are included in the coordinate representation (see the following) by the method described in Appendix B. The effective interaction in the pp channel and the gap equation within the HF+BCS approximation are determined by the formulas of Appendix A of Ref. [23] with $\mathcal{F}^{\xi}(r) = \frac{1}{2} V_0$ (see also Appendix C of the present paper).

B. Dynamical pairing effects in QRPA and QTBA

One of the important questions arising in the QRPA and QTBA calculations is the question of completeness of the configuration space. The size of the basis in this space has an impact practically on all the calculated quantities. In particular, configurations with a particle in the continuum are responsible for the formation of the escape widths of the resonances. The well-known method to include these configurations on the RPA level is the use of the coordinate representation within the Green function formalism (see Ref. [27]). We use this method in our approach as described in Ref. [23]. However, incorporation of the pp-channel contributions in the coordinate representation leads to considerable numerical difficulties. At the same time, the pp-channel contributions (so-called dynamical pairing effects) are very important in the calculations of 0^+ excitations in the open-shell nuclei, primarily because of the problem of the 0^+ spurious state. For this reason we have developed a combined method, which is a modification of the so-called (r, λ) representation proposed in Ref. [28] for the QRPA problem. Within this method only the ph channel is treated in the coordinate space; the dynamical pairing effects are included in the discrete basis representation.

Consider the general case of the QTBA. By taking into account the decomposition of Eq. (2) one can rewrite Eq. (1) in the form

$$R^{\mathrm{eff}}(\omega) = A^{(\mathrm{res+pp})}(\omega) - A^{(\mathrm{res+pp})}(\omega)\, \mathcal{F}^{(\mathrm{ph})}\, R^{\mathrm{eff}}(\omega), \tag{18}$$

where propagator $A^{(\mathrm{res+pp})}(\omega)$ is a solution of the equation

$$A^{(\mathrm{res+pp})}(\omega) = A(\omega) - A(\omega)\,\mathcal{F}^{(\mathrm{pp})}A^{(\mathrm{res+pp})}(\omega). \quad (19)$$

In the present work we use the version of the QTBA in which the ground-state correlations caused by the QPC are neglected. In this case the correlated propagator $A(\omega)$ is defined by the equation

$$A(\omega) = \tilde{A}(\omega) - \tilde{A}(\omega)\,\bar{\Phi}(\omega)\,A(\omega), \quad (20)$$

where $\tilde{A}(\omega)$ is the uncorrelated QRPA propagator,

$$\bar{\Phi}(\omega) = \Phi^{(\mathrm{res})}(\omega) - \Phi^{(\mathrm{res})}(0), \quad (21)$$

and $\Phi^{(\mathrm{res})}(\omega)$ is a resonant part of the interaction amplitude responsible for the QPC in our model (see Refs. [22,23] for details). Combining Eqs. (19) and (20) leads to the new equation for $A^{(\mathrm{res+pp})}(\omega)$:

$$A^{(\mathrm{res+pp})}(\omega) = \tilde{A}(\omega) - \tilde{A}(\omega)[\bar{\Phi}(\omega) + \mathcal{F}^{(\mathrm{pp})}]A^{(\mathrm{res+pp})}(\omega). \quad (22)$$

As a result we find that the pp-channel contributions can be included by modification of the equation for the correlated propagator [i.e., by replacing Eq. (20) by Eq. (22)]. The modification is reduced to the additional term $\mathcal{F}^{(\mathrm{pp})}$ added to the amplitude $\bar{\Phi}(\omega)$. The respective equations in terms of the reduced matrix elements are derived in Appendix C. It is worth noting that the QPC in the QTBA is included both in the ph channel and in the pp channel because there is no difference between these channels in the representation of the single-quasiparticle basis functions in the doubled space ($\tilde{\psi}_1$; see Ref. [23]) used in Eqs. (19), (20), and (22). This is true for both the system of equations given by Eqs. (1) and (20) and the system given by Eqs. (18) and (22).

In practice Eq. (18) for $R^{\mathrm{eff}}(\omega)$ is solved in the coordinate representation (to take into account the single-particle continuum), whereas Eq. (22) is solved in the restricted discrete basis representation. This fact greatly simplifies the problem as compared with the initial Eq. (1) in which both the ph-channel contribution and the pp-channel one are included in the coordinate representation. At the same time, the use of the restricted discrete basis representation for the pp channel is fully consistent with the BCS approximation in which the gap equation is solved in the same restricted basis.

The general scheme described here ensures that the energy of the 0^+ spurious state (the so-called ghost state) is equal to zero both in the QRPA and in the QTBA. However, there still remains the following problem: In the QTBA the ghost state can be fragmented owing to its coupling to the $2q \otimes$ phonon configurations, despite the energy of the dominant ghost state being equal to zero. This can lead to the spurious states at low energies. The appearance of these states can distort respective strength functions. In particular, these fragmented spurious states will produce nonzero response to the particle-number operator, which has to be exactly equal to zero in a correct theory (as, for instance, in the QRPA including the pp channel that was proved by Migdal [29]). In the present calculations this additional problem arising in the QTBA is solved with the help of a special projection technique, which will be described in a forthcoming publication.

III. CALCULATIONS OF THE GIANT MONOPOLE RESONANCE IN THE TIN ISOTOPES

A. Numerical details

The method just described has been applied to calculate the strength distributions of the isoscalar giant monopole resonance in the even-A tin isotopes ($A = 112$–124) that were recently measured experimentally at RCNP (see Ref. [18]). The ground-state properties of these nuclei were calculated within the HF+BCS approximation using T5 and T6 Skyrme forces with the parameters taken from Ref. [24] including the pairing-force strength $V_0 = -210$ MeV fm^3 in Eq. (7). The same forces were used to calculate the effective residual interaction as described in Sec. II. For all tin isotopes under consideration, the pairing window for the neutrons contains 22 states including all the discrete states and one ($1i_{13/2}$) or two ($1h_{9/2}$ and $1i_{13/2}$) quasidiscrete states. The criterion to select quasidiscrete states is described in Ref. [23].

To calculate the strength function of the ISGMR, Eq. (1) for the effective response function $R^{\mathrm{eff}}(\omega)$ was solved by using its reduction to the system of Eqs. (18) and (22). The strength function $S(E)$ is determined by $R^{\mathrm{eff}}(\omega)$ via the formulas

$$S(E) = -\frac{1}{\pi}\,\mathrm{Im}\,\Pi(E + i\Delta), \quad (23)$$

$$\Pi(\omega) = -\frac{1}{2}\sum_{1234}(eV^0)^*_{21}\,R^{\mathrm{eff}}_{12,34}(\omega)(eV^0)_{43}, \quad (24)$$

where $\Pi(\omega)$ is the nuclear polarizability, E is an excitation energy, Δ is a smearing parameter, V^0 is an external field, and e is an effective charge operator. In the case of the isoscalar 0^+ excitations the one-body operator eV^0 is proportional to the identity matrices both in the spin and in the isospin indices. Its radial dependence is taken in our calculations in the form $eV^0 = r^2$. The smearing parameter was taken to be equal to 500 keV, which approximately corresponds to the experimental resolution for the data presented in Ref. [18].

In the calculation of the QTBA correlated propagator $A(\omega)$ entering Eq. (1), the valence zone for the neutrons coincides with the pairing window. The valence zone for the protons contains 20 states including all the discrete states and several quasidiscrete states as described in Ref. [23]. Let us emphasize that the restricted valence zone is used only in the calculation of the discrete part of the propagator $A(\omega)$ including QPC effects and in the calculation of the phonons (see the following). In the ISGMR calculations, the configurations with the particle in the continuum are included completely in the RPA-like part of $A(\omega)$ (see Ref. [23] for details).

The set of phonons in the QTBA calculations included collective modes with values of the spin L in the interval $2 \leqslant L \leqslant 9$ and with natural parity $\pi = (-1)^L$. The phonon characteristics were calculated within the QRPA by using configuration space restricted by the valence zone just described. The maximal energy of the phonon was adopted to be equal to the value 10 MeV, which is approximately equal to the nucleon separation energy for the given tin isotopes. The second criterion to include the phonon into the phonon space was its reduced transition probability $B(EL)$, which should be more than 10% of the maximal $B(EL)$ for the given spin. According to these

TABLE I. Mean energies and Lorentzian-fit parameters for the ISGMR strength distributions in the even-A $^{112-124}$Sn isotopes. The mean energies are calculated for the 10.5–20.5 MeV energy interval. Theoretical results are obtained within the QRPA and the QTBA, which is an extension of the QRPA including quasiparticle-phonon coupling. The self-consistent HF+BCS calculational scheme based on the T5 ($K_\infty = 202$ MeV) and T6 ($K_\infty = 236$ MeV) Skyrme forces is used. The RPA results for ^{100,132}Sn are shown for comparison. Experimental values are taken from Ref. [18] (RCNP).

	Method	Force	$\sqrt{m_1/m_{-1}}$ (MeV)	m_1/m_0 (MeV)	$\sqrt{m_3/m_1}$ (MeV)	E_{GMR} (MeV)	Γ (MeV)
^{100}Sn	RPA	T6	17.2	17.3	17.5	17.5	1.9
	RPA	T5	16.0	16.1	16.3	16.1	1.7
^{112}Sn	QRPA	T6	17.0	17.1	17.3	17.3	1.9
	QRPA	T5	15.8	15.9	16.1	15.9	1.8
	QTBA	T5	15.7	15.8	16.2	15.8	3.7
	Exp.		16.1 ± 0.1	16.2 ± 0.1	16.7 ± 0.2	16.1 ± 0.1	4.0 ± 0.4
^{114}Sn	QRPA	T6	16.9	17.0	17.2	17.3	2.0
	QRPA	T5	15.7	15.8	16.0	15.8	1.8
	QTBA	T5	15.6	15.7	16.1	15.7	3.7
	Exp.		15.9 ± 0.1	16.1 ± 0.1	16.5 ± 0.2	15.9 ± 0.1	4.1 ± 0.4
^{116}Sn	QRPA	T6	16.8	16.9	17.1	17.2	2.1
	QRPA	T5	15.6	15.6	15.9	15.7	1.9
	QTBA	T5	15.5	15.6	16.0	15.6	3.8
	Exp.		15.7 ± 0.1	15.8 ± 0.1	16.3 ± 0.2	15.8 ± 0.1	4.1 ± 0.3
^{118}Sn	QRPA	T6	16.6	16.7	17.0	17.1	2.1
	QRPA	T5	15.4	15.5	15.8	15.6	2.0
	QTBA	T5	15.4	15.5	15.9	15.5	3.9
	Exp.		15.6 ± 0.1	15.8 ± 0.1	16.3 ± 0.1	15.6 ± 0.1	4.3 ± 0.4
^{120}Sn	QRPA	T6	16.5	16.6	16.9	17.0	2.2
	QRPA	T5	15.3	15.4	15.7	15.5	2.1
	QTBA	T5	15.3	15.4	15.8	15.3	3.9
	Exp.		15.5 ± 0.1	15.7 ± 0.1	16.2 ± 0.2	15.4 ± 0.2	4.9 ± 0.5
^{122}Sn	QRPA	T6	16.4	16.5	16.8	16.9	2.3
	QRPA	T5	15.2	15.3	15.5	15.4	2.1
	QTBA	T5	15.1	15.3	15.7	15.2	3.8
	Exp.		15.2 ± 0.1	15.4 ± 0.1	15.9 ± 0.2	15.0 ± 0.2	4.4 ± 0.4
^{124}Sn	QRPA	T6	16.2	16.4	16.7	16.7	2.3
	QRPA	T5	15.0	15.1	15.4	15.2	2.2
	QTBA	T5	15.0	15.2	15.5	15.1	3.8
	Exp.		15.1 ± 0.1	15.3 ± 0.1	15.8 ± 0.1	14.8 ± 0.2	4.5 ± 0.5
^{132}Sn	RPA	T6	15.7	15.8	16.1	16.0	2.5
	RPA	T5	14.4	14.5	14.8	14.5	2.2

criteria, the total number of phonons included in the QTBA calculations is equal to 21 for ^{112}Sn, 19 for ^{114}Sn, 23 for ^{116}Sn, 26 for ^{118}Sn, 29 for ^{120}Sn, 27 for ^{122}Sn, and 31 for ^{124}Sn.

To describe correctly effects of a fragmentation of the resonances in the QTBA arising from the QPC it is very important to use the phonon space with the phonon characteristics close to the experimental ones. However, neither the T5 nor the T6 Skyrme force provides a satisfactory description of the experimental energies and transition probabilities within the self-consistent QRPA scheme presented in Sec. II. For this reason, in the calculation of the phonons (and only in this calculation) we have used the QRPA scheme that is self-consistent only on the mean-field level. More specifically, the mean field was calculated within the HF+BCS approximation based on the T5 Skyrme force, whereas the effective residual interaction was taken in the form of the Landau-Migdal zero-range force with the standard set of the parameters (see, e.g., Ref. [30]), except for the parameter f_{ex}. This parameter was adjusted for the each nucleus to reproduce the experimental energies of the 2^+_1 and 3^-_1 levels. As a result, the parameter f_{ex} takes the values in the interval -1.54 ± 0.11 for phonons with positive parity and the values in the interval -1.83 ± 0.06 for phonons with negative parity.

B. Results and discussion

The results for the ISGMR strength distributions in the even-A $^{112-124}$Sn isotopes are presented in Fig. 1 and in Table I. The mean energies of the ISGMR shown in the tables are

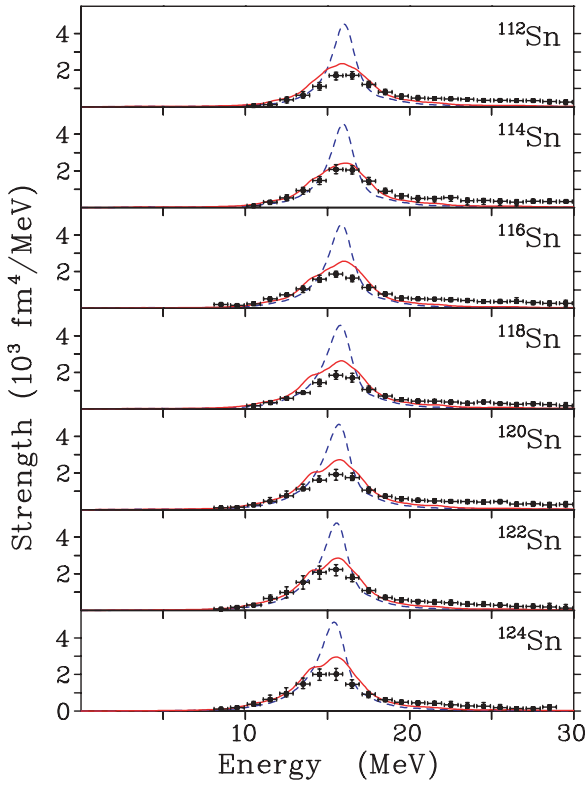

FIG. 1. (Color online) Isoscalar giant monopole resonance in the even-A $^{112-124}$Sn isotopes calculated within QRPA (dashed line) and QTBA (solid line). The results are obtained within the self-consistent HF+BCS approach based on the T5 Skyrme force. The smearing parameter Δ is equal to 500 keV. Experimental data (solid squares) are taken from Ref. [18].

defined via the ratios of the energy-weighted moments m_k determined as

$$m_k = \int_{E_1}^{E_2} E^k S(E)\, dE. \tag{25}$$

The energy interval limited by $E_1 = 10.5$ MeV and $E_2 = 20.5$ MeV was taken to be the same as in Ref. [18]. The peak energies $E_{\rm GMR}$ and the widths Γ of the ISGMR were obtained from the Lorentzian fit of the calculated functions $S(E)$. As can be seen from Table I, the agreement of the theoretical results with the experimental mean and peak energies in the case of the T5 Skyrme force is fairly good both in the QRPA and in the QTBA. The fact that the mean and peak energies obtained in the QRPA and in the QTBA are very close to each other is explained by the subtraction procedure used in our calculations (see Eq. (21) and Ref. [23] for a discussion). The main reason for the agreement with experiment in this case is the comparatively low value of the incompressibility modulus of INM ($K_\infty = 202$ MeV) produced by the T5 Skyrme-force parametrization. The other parametrizations with K_∞ around 240 MeV give mean energies of the ISGMR that are too large for the considered tin isotopes as compared with the experimental values.

For comparison, in Table I we show the QRPA results obtained with the T6 Skyrme force ($K_\infty = 236$ MeV). As can be seen, the T6 peak energies $E_{\rm GMR}$ are greater than the experimental values for the tin isotopes by 1.2–1.9 MeV. This fact agrees with the results of Ref. [31], where the relativistic RPA calculations based on the force with $K_\infty = 230$ MeV were shown to consistently overestimate the centroid energies of the ISGMR in the same tin isotopes.

These results can be expressed in terms of the Skyrme force parameter α, which determines the density-dependence power of the effective nuclear forces. Namely, according to Eq. (17) we find that the value $\alpha = 1/6$ leads to the best description of the experimental data for the tin isotopes in our calculations in which the Skyrme forces with $m^* = m$ were used. On the other hand, from Eqs. (14)–(16) it follows that if we fix the values k_F, B/A, and K_∞ while decreasing the effective mass we get a smaller value of the parameter α. In particular, putting $K_\infty = 202$ MeV and $m^* = 0.8\, m$ we obtain $\alpha \approx 0.07$, which is substantially less than the conventional values of this parameter. As $m^* \to m^*_{\rm crit}$, where $m^*_{\rm crit} \approx 0.72\, m$, the parameter α tends to the singular point $\alpha = 0$, where, in the general case, the aforementioned conditions on the values of k_F, B/A, and K_∞ cannot be satisfied simultaneously. This fact indicates that the value $m^* = m$ is a fairly reasonable choice in the case when the INM incompressibility modulus is set to $K_\infty = 202$ MeV.

It is worth noting that the value $K_\infty = 202$ MeV corresponding to the T5 Skyrme force ($\alpha = 1/6$) lies within the interval 210 ± 30 MeV, which was long considered as the nonrelativistic estimate for this quantity. The recent results [11,12] inferring K_∞ to be 230–240 MeV were obtained within the RPA and the constrained HF method on the basis of experimental data in fact for only the one nucleus ^{208}Pb. Our RPA result for the mean energy m_1/m_0 obtained with the T6 Skyrme force ($K_\infty = 236$ MeV and $\alpha = 1/3$) also nicely agrees with TAMU experimental data [32] for this nucleus (see Table II). At the same time, the T5 force gives the RPA value m_1/m_0 for ^{208}Pb that is smaller by 1.3 MeV as compared with the value from this experiment. Note, however, that the ISGMR data even for the well-studied nucleus ^{208}Pb are not quite unambiguous. In particular, the experimental value of the ISGMR peak energy in ^{208}Pb measured in the RCNP experiment [33] is smaller by 0.6 MeV as compared with the value m_1/m_0 from Ref. [32] and lies between the RPA values of $E_{\rm GMR}$ obtained with the T5 and T6 Skyrme forces.

In Table II, we also show the QRPA results for ^{90}Zr and ^{144}Sm nuclei in comparison with the available ISGMR data. The experimental value of the ISGMR peak energy in ^{90}Zr obtained by the RCNP [33] is fairly well reproduced by the calculation with the T5 Skyrme force. In the other cases, the experimental values lie between ones calculated with the T5 and T6 forces. These results show that the question of the precise value of K_∞ is not resolved within the framework of our approach.

In contrast to the mean energies, the QRPA and the QTBA give substantially different values for the width of the ISGMR. It is well known that the spreading width $\Gamma^\downarrow$ is a considerable part of the total width of the giant resonance. The QRPA does not produce $\Gamma^\downarrow$, whereas in the QTBA it is formed by the 2q $\otimes$ phonon configurations. This is the reason why the QRPA strongly underestimates the experimental values of Γ, while reasonably good agreement is achieved in the QTBA.

TABLE II. The same as in Table I, but for the (Q)RPA calculations in ^{90}Zr, ^{144}Sm, and ^{208}Pb nuclei. The mean energies are obtained for the 5–25 MeV energy interval. Experimental data are taken from Refs. [33,34] (RCNP, Osaka University) and Refs. [1,32] (TAMU, Texas A&M University).

	Method	Force	$\sqrt{m_1/m_{-1}}$ (MeV)	m_1/m_0 (MeV)	$\sqrt{m_3/m_1}$ (MeV)	$E_{\rm GMR}$ (MeV)	Γ (MeV)
^{90}Zr	QRPA	T6	18.0	18.2	18.6	18.0	3.0
	QRPA	T5	16.6	16.8	17.2	16.5	2.0
	Exp. [33]					16.6 ± 0.1	4.9 ± 0.2
	Exp. [1]			17.89 ± 0.20			
^{144}Sm	QRPA	T6	15.8	16.0	16.4	15.8	2.0
	QRPA	T5	14.6	14.7	15.1	14.5	1.5
	Exp. [34]					$15.30^{+0.11}_{-0.12}$	$3.71^{+0.12}_{-0.63}$
	Exp. [32]			15.40 ± 0.30			3.40 ± 0.20
^{208}Pb	RPA	T6	13.8	14.0	14.5	13.9	1.9
	RPA	T5	12.6	12.7	13.2	12.6	1.6
	Exp. [33]					13.4 ± 0.2	4.0 ± 0.4
	Exp. [32]			13.96 ± 0.20			2.88 ± 0.20

To investigate the nature of the dependence of the ISGMR mean energies on the neutron excess $(N - Z)$ we calculated the unperturbed $0^+_{\rm IS}$ response by substituting the (Q)RPA uncorrelated propagator $\tilde{A}(\omega)$ in Eq. (24) instead of $R^{\rm eff}(\omega)$. This response corresponds to the independent quasiparticle model (IQM). The results are presented in Table III in comparison with the (Q)RPA results obtained in the same energy interval of 10–30 MeV. This interval was chosen to exclude contribution of the low-lying strength arising in the IQM response. As can be seen from Table III, the $(N - Z)$ dependence of the (Q)RPA mean energies practically follows the dependence of the IQM energies. In particular, the difference between the m_1/m_0 values for ^{112}Sn and ^{124}Sn in the QRPA is equal to 0.8 MeV and approximately the same difference 0.9 MeV is obtained in the IQM calculation. Since the poles of the uncorrelated propagator $\tilde{A}(\omega)$ are equal to the sums of the quasiparticle energies $E_{(1)} + E_{(2)}$ [see Eq. (C3)], this result means that the $(N - Z)$ dependence of the ISGMR mean energies is mainly determined by the level density of the single-quasiparticle spectrum. Including the residual interaction in the (Q)RPA, we obtain the following redistribution of the isoscalar monopole strength: The low-lying part of the strength disappears, and the mean energy of the high-lying states (which form the ISGMR) is reduced by approximately 2.4 MeV.

TABLE III. Mean energies for the $0^+_{\rm IS}$ strength distributions in the even-A $^{100,112-124,132}$Sn isotopes calculated for the 10–30 MeV energy interval within the self-consistent HF+BCS approach based on the T5 Skyrme force. See text for details.

	Method	$\sqrt{m_1/m_{-1}}$ (MeV)	m_1/m_0 (MeV)	$\sqrt{m_3/m_1}$ (MeV)
^{100}Sn	IQM	19.1	19.3	19.9
	RPA	16.3	16.4	16.8
^{112}Sn	IQM	18.5	18.7	19.4
	QRPA	16.1	16.2	16.7
^{114}Sn	IQM	18.3	18.5	19.3
	QRPA	15.9	16.1	16.6
^{116}Sn	IQM	18.1	18.4	19.1
	QRPA	15.8	15.9	16.5
^{118}Sn	IQM	17.9	18.2	19.0
	QRPA	15.7	15.8	16.3
^{120}Sn	IQM	17.8	18.1	18.9
	QRPA	15.5	15.7	16.2
	RPA	15.2	15.4	15.9
^{122}Sn	IQM	17.6	17.9	18.7
	QRPA	15.4	15.5	16.1
^{124}Sn	IQM	17.5	17.8	18.6
	QRPA	15.2	15.4	15.9
^{132}Sn	IQM	17.1	17.4	18.2
	RPA	14.6	14.7	15.2

In Table III, we also include the ISGMR mean energies obtained within the RPA for the ^{120}Sn nucleus. In this calculation, the pairing correlations are neglected both in the mean field and in the residual interaction. The respective strength function is shown in Fig. 2 in comparison with the IQM and QRPA strength functions. These results demonstrate that the influence of the pairing correlations on the ISGMR mean energies is appreciable. In the QRPA, where the pairing

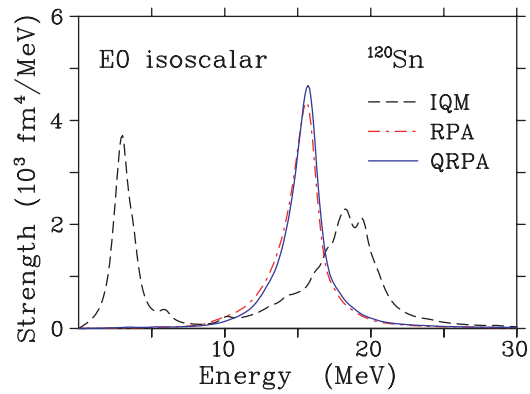

FIG. 2. (Color online) Isoscalar $E0$ response in ^{120}Sn calculated within the independent quasiparticle model (IQM, dashed line), RPA (dashed-dotted line), and QRPA (solid line), making use of the T5 Skyrme force. See text for details. The smearing parameter Δ is equal to 500 keV.

correlations are included, the mean energies increase by 0.27 MeV as compared with the RPA. On the other hand, the QRPA mean energies calculated with the T6 Skyrme force for ^{120}Sn in the energy interval 10–30 MeV are greater than the respective T5 values listed in Table III by 1.37 MeV. Since the difference between the values of K_∞ for the T5 and T6 forces is equal to 34 MeV, the shift of the ISGMR mean energies by 0.27 MeV in this nucleus corresponds to $\delta K_\infty \approx 7$ MeV.

Note also that the energy shift induced by the pairing correlations in the considered tin isotopes is greater than the total shift caused by the spin-orbital and the Coulomb components of the effective interaction. In our previous calculations of the ISGMR (see Ref. [35]) these components were not included. As a result, the calculated ISGMR mean energies in the $^{112-124}$Sn nuclei were shifted upward by about 0.1–0.2 MeV. This relatively small difference is a consequence of the near cancellation between the spin-orbital and the Coulomb contributions in the interaction (see also Ref. [36], where these effects were investigated in more detail).

IV. CONCLUSIONS

In the paper the results of the theoretical analysis of the ISGMR strength distributions in the even-A $^{112-124}$Sn isotopes were presented. The calculations were performed within two microscopic models: the quasiparticle random phase approximation and the quasiparticle time blocking approximation, which is an extension of the QRPA including quasiparticle-phonon coupling. We used a calculational scheme based on the HF+BCS approximation, which is fully self-consistent on the RPA level. The self-consistent mean field and the effective interaction (including the spin-orbital and the Coulomb contributions in both quantities) were derived from the Skyrme energy functional. In the calculations, two Skyrme force parametrizations were used. The T5 parametrization with comparatively low value of the incompressibility modulus of infinite nuclear matter ($K_\infty = 202$ MeV) allowed us to achieve good agreement with the experimental data for tin isotopes within the QTBA including resonance widths. However, this parametrization underestimates the experimental ISGMR mean energy for the ^{208}Pb nucleus, which is usually used in the fit of the Skyrme force parameters. The T6 Skyrme force with $K_\infty = 236$ MeV nicely reproduces the ISGMR mean energy for ^{208}Pb but overestimates the energies for $^{112-124}$Sn isotopes by more than one MeV. The experimental data on the ISGMR energies in ^{90}Zr and ^{144}Sm nuclei lie between the values calculated by us with the T5 and T6 forces, though the T6 Skyrme force leads on average to a better description of the experiment. On the whole, these results do not allow us to decrease the ambiguity in the value of K_∞ as compared with the previous known estimates. Note, however, that the main goal of our work is not to solve the problem of the nuclear matter incompressibility but to find under which conditions one can obtain reasonable description of the experimental data for the considered tin isotopes within the framework of the self-consistent approach including correlations beyond the QRPA.

ACKNOWLEDGMENTS

V.T. thanks the staff of the Institut für Kernphysik at the Forschungszentrum Jülich for their hospitality during the completion of this work. This work was supported by the Deutsche Forschungsgemeinschaft under Grant No. 436 RUS 113/806/0-1 and by the Russian Foundation for Basic Research under Grant No. 05-02-04005-DFG_a. V.T., E.L., and N.L. acknowledge financial support from the Russian Federal Agency of Education under Project No. 2.1.1/4779.

APPENDIX A: SPIN-SCALAR COMPONENTS OF THE EFFECTIVE RESIDUAL INTERACTION IN THE COORDINATE REPRESENTATION

Equations (5) and (13) lead to the following explicit form of the spin-scalar components of the effective residual interaction in the ph channel:

$$\begin{aligned}\mathcal{F}^{(\mathrm{ph})}_{0,\,nn}(\boldsymbol{r},\boldsymbol{r}') = {} & \left(\tfrac{1}{2}\,t_0\,(1-x_0) + \tfrac{1}{12}\,t_3\left\{\left(1+\tfrac{1}{2}\,x_3\right)(1+\alpha)\right.\right.\\ & \times(2+\alpha)\,\rho^\alpha - \left(x_3+\tfrac{1}{2}\right)\left[2\rho^\alpha + 4\alpha\rho_n\rho^{\alpha-1}\right.\\ & \left.\left.+\,\alpha(\alpha-1)\left(\rho_n^2+\rho_p^2\right)\rho^{\alpha-2}\right]\right\}\Big)\,\delta(\boldsymbol{r}-\boldsymbol{r}')\\ & + \tfrac{3}{16}\,[t_2\,(1+x_2) - t_1\,(1-x_1)]\Delta\,\delta(\boldsymbol{r}-\boldsymbol{r}'),\end{aligned} \tag{A1}$$

$$\begin{aligned}\mathcal{F}^{(\mathrm{ph})}_{0,\,np}(\boldsymbol{r},\boldsymbol{r}') = {} & \left(t_0\left(1+\tfrac{1}{2}\,x_0\right) + \tfrac{1}{12}\,t_3\left\{\left(1+\tfrac{1}{2}\,x_3\right)(1+\alpha)\right.\right.\\ & \times(2+\alpha)\,\rho^\alpha - \left(x_3+\tfrac{1}{2}\right)\alpha\,[(\alpha+1)\rho^\alpha\\ & \left.\left.-\,2(\alpha-1)\rho_n\,\rho_p\,\rho^{\alpha-2}]\right\}\Big)\,\delta(\boldsymbol{r}-\boldsymbol{r}')\\ & + \tfrac{1}{8}\left[t_2\left(1+\tfrac{1}{2}x_2\right) - 3t_1\left(1+\tfrac{1}{2}x_1\right)\right]\Delta\,\delta(\boldsymbol{r}-\boldsymbol{r}').\end{aligned} \tag{A2}$$

The formulas for the components $\mathcal{F}^{(\mathrm{ph})}_{0,\,pp}$ and $\mathcal{F}^{(\mathrm{ph})}_{0,\,pn}$ are obtained from Eqs. (A1) and (A2) by replacing indices n by p and p by n and by adding the Coulomb interaction to $\mathcal{F}^{(\mathrm{ph})}_{0,\,pp}$. The radial parts of these functions entering the QTBA equation (33) of Ref. [23] are defined as follows:

$$\begin{aligned}\mathcal{F}^{J\,(\mathrm{ph,ph})}_{L0q,\,L'0q'}(r,r') = {} & \frac{\delta_{LL'}}{2L+1}\sum_M \int d\boldsymbol{n}\,d\boldsymbol{n}'\,Y^*_{LM}(\boldsymbol{n})\\ & \times\mathcal{F}^{(\mathrm{ph})}_{0,\,qq'}(\boldsymbol{r},\boldsymbol{r}')Y_{LM}\,(\boldsymbol{n}').\end{aligned} \tag{A3}$$

APPENDIX B: SPIN-ORBITAL COMPONENTS IN THE CASE OF THE 0^+ EXCITATIONS

To include the spin-orbital components of the effective residual interaction in the QRPA and the QTBA equations written in the coordinate representation one has to extend the set of quantum numbers related to the angular momentum. If we restrict ourselves to the case of the 0^+ excitations, the following procedure is applicable. Using the notation of Ref. [23], we formally introduce one additional value of the quantum number S entering the set $\{J, L, S\}$, where J is the total angular momentum of the excited state, $L = J$ for the natural-parity excitations, and $S = 0, 1$. Namely, we

introduce the value $S = 2$ for the spin-orbital components of the quantities entering the QTBA equation (33) of Ref. [23]. Thus, in the case of the 0^+ excitations we have $J = L = 0$ and $S = 0, 2$. The components of the correlated propagator $A^{J(\mathrm{ph,ph})}_{LSq,L'S'q'}(r, r'; \omega)$ with $S, S' = 0, 2$ are defined by Eqs. (41)–(44) of Ref. [23] in which we formally set

$$\langle\, jl \,||\, T_{002} \,||\, jl \,\rangle = \langle l\sigma \rangle_{jl} \,\langle\, jl \,||\, T_{000} \,||\, jl \,\rangle, \tag{B1}$$

where $\langle\, jl \,||\, T_{JLS} \,||\, j'l' \,\rangle$ on the right-hand side of Eq. (B1) is the reduced matrix element of the spherical tensor operator and

$$\langle l\sigma \rangle_{jl} = j(j+1) - l(l+1) - \tfrac{3}{4}. \tag{B2}$$

The respective components of the interaction $\mathcal{F}^{(\mathrm{ph})}_{SS',qq'}(r, r') = \mathcal{F}^{J=0\,(\mathrm{ph,ph})}_{0Sq,0S'q'}(r, r')$ in Eq. (33) of Ref. [23] are defined as follows:

$$\begin{aligned}\mathcal{F}^{(\mathrm{ph})}_{02,\,qq'}(r, r') &= \mathcal{F}^{(\mathrm{ph})}_{20,\,q'q}(r', r) \\ &= -\frac{1}{2}\, W_0\,(1 + \delta_{qq'})\,\frac{1}{r'r^2}\,\frac{\partial}{\partial r}\,\delta(r - r'), \qquad \text{(B3)}\\ \mathcal{F}^{(\mathrm{ph})}_{22,\,qq'}(r, r') &= -\frac{1}{8}\,[t_1x_1 + t_2x_2 - \delta_{qq'}(t_1 - t_2)] \\ &\quad \times \frac{1}{(rr')^2}\,\delta(r - r'). \qquad \text{(B4)}\end{aligned}$$

To check the accuracy of our method we have calculated the ISGMR mean energy $\sqrt{m_1/m_{-1}}$ in three nuclei, ^{100}Sn, ^{120}Sn, and ^{208}Pb, within the RPA and have compared the results with the values obtained using the constrained HF (CHF) method described in Ref. [3] (see also Ref. [10] for details of our calculational scheme). In the calculations the T5 Skyrme force was used. The CHF method yields the values 16.25 MeV for ^{100}Sn, 15.08 MeV for ^{120}Sn, and 12.65 MeV for ^{208}Pb. The energy-weighted moments m_1 and m_{-1} in the RPA were calculated by the method described in Ref. [37]. According to this method, the values of the moments m_k for the odd k are defined by the formula

$$m_k = \frac{\mathrm{sgn}(k)}{2N}\,\mathrm{Re}\left(\sum_{n=1}^{N} \Omega_n^{k+1}\,\Pi(\Omega_n)\right), \tag{B5}$$

where $\Pi(\omega)$ is defined by Eq. (24) and

$$\Omega_n = \Omega\, e^{i(2n-1)\pi/4N}. \tag{B6}$$

As $N \to \infty$ and $\Omega \to \infty$ for $k > 0$ ($\Omega \to 0$ for $k < 0$) this definition coincides with Eq. (25) for the case $E_1 = 0$, $E_2 = \infty$, and $\Delta \to +0$ in Eq. (23) (i.e., for the case corresponding to the CHF result). In our calculations, the following parameters entering Eqs. (B5) and (B6) were taken: $N = 7$, $\Omega = 150$ MeV for m_1, and $\Omega = 0.1$ MeV for m_{-1}. The RPA equation was solved in coordinate space using a mesh size of 0.2 fm. In this way we have obtained in the self-consistent RPA for all three nuclei the values $\sqrt{m_1/m_{-1}}$ coinciding with the CHF results listed here within the accuracy of our CHF calculations (i.e., with a relative error of about 10^{-4}). Note that the energy-weighted sum rule represented by the moment m_1 is exhausted in these RPA calculations with the same relative error of about 10^{-4}.

APPENDIX C: MODIFICATION OF THE QTBA EQUATIONS INCLUDING CONTRIBUTION OF THE PARTICLE-PARTICLE CHANNEL IN TERMS OF THE REDUCED MATRIX ELEMENTS

In the detailed form using the notation of Ref. [23] for the reduced matrix elements, our method to include the pp-channel contribution in the QTBA equations consists of the following. In Eq. (33) of Ref. [23] only the ph channel is kept, but in Eq. (42) for $A^{J\,(\mathrm{ph,ph})\,LS,L'S'}_{[12,34]}(r, r'; \omega)$ the matrix element $A^{J}_{[12,34]}(\omega)$ is replaced by $A^{J\,(\mathrm{res+pp})}_{[12,34]}(\omega)$, where

$$A^{J\,(\mathrm{res+pp})}_{[12,34]}(\omega) = \delta_{\eta_1,-\eta_2}\,\delta_{\eta_3,-\eta_4}\,A^{J\,(\mathrm{res+pp})}_{(12)\eta_1,\,(34)\eta_3}(\omega). \tag{C1}$$

Propagator $A^{J\,(\mathrm{res+pp})}_{(12)\eta,\,(34)\eta'}(\omega)$ is a solution of the equation

$$\begin{aligned}A^{J\,(\mathrm{res+pp})}_{(12)\eta,\,(34)\eta'}(\omega) &= \tilde{A}^{J}_{(12)\eta,\,(34)\eta'}(\omega) \\ &\quad + \sum_{\eta''}\sum_{(56)} \theta_{(65)}\,\bar{\mathcal{K}}^{J\,(\mathrm{res+pp})}_{(12)\eta,\,(56)\eta''}(\omega) \\ &\quad \times A^{J\,(\mathrm{res+pp})}_{(56)\eta'',\,(34)\eta'}(\omega), \qquad \text{(C2)}\end{aligned}$$

where

$$\tilde{A}^{J}_{(12)\eta,\,(34)\eta'}(\omega) = -\frac{\eta\,\delta_{\eta,\eta'}\big[\delta_{(13)}\,\delta_{(24)} + s^{J}_{(12)}\,\delta_{(14)}\,\delta_{(23)}\big]}{2\,(\omega - \eta\,[E_{(1)} + E_{(2)}])}, \tag{C3}$$

$$\bar{\mathcal{K}}^{J\,(\mathrm{res+pp})}_{(12)\eta,\,(34)\eta'}(\omega) = \frac{\eta\,\big[\bar{\Phi}^{J\,(\mathrm{res+pp})}_{(12)\eta,\,(34)\eta'}(\omega) + s^{J}_{(12)}\,\bar{\Phi}^{J\,(\mathrm{res+pp})}_{(21)\eta,\,(34)\eta'}(\omega)\big]}{\omega - \eta\,[E_{(1)} + E_{(2)}]}, \tag{C4}$$

$$\bar{\Phi}^{J\,(\mathrm{res+pp})}_{(12)\eta,\,(34)\eta'}(\omega) = \sum_{\eta_1\eta_2\eta_3\eta_4} \delta_{\eta_1,\,\eta}\,\delta_{\eta_2,-\eta}\,\delta_{\eta_3,\,\eta'}\,\delta_{\eta_4,-\eta'}\,\bar{\Phi}^{J\,(\mathrm{res+pp})}_{[12,34]}(\omega), \tag{C5}$$

$$\bar{\Phi}^{J\,(\mathrm{res+pp})}_{[12,34]}(\omega) = \Phi^{J\,(\mathrm{res})}_{[12,34]}(\omega) - \Phi^{J\,(\mathrm{res})}_{[12,34]}(0) + \mathcal{F}^{J(\mathrm{pp})}_{[12,34]}, \tag{C6}$$

and $s^{J}_{(12)} = (-1)^{J+l_1-l_2+j_1-j_2}$. The order-bounding factors $\theta_{(21)}$ in Eq. (C2) are defined as follows: $\theta_{(21)} = 1$ if the ordinal number of the state (1) is less than the number of (2) [(1) < (2)], $\theta_{(21)} = \frac{1}{2}$ if (1) = (2), and $\theta_{(21)} = 0$ if (1) > (2). The interaction amplitude $\Phi^{J\,(\mathrm{res})}_{[12,34]}(\omega)$ responsible for the QPC is defined by Eq. (B14) of Ref. [23]. Introducing the notation

$$\mathcal{F}^{J(\mathrm{pp})}_{(12)\eta,\,(34)\eta'} = \sum_{\eta_1\eta_2\eta_3\eta_4} \delta_{\eta_1,\,\eta}\,\delta_{\eta_2,-\eta}\,\delta_{\eta_3,\,\eta'}\,\delta_{\eta_4,-\eta'}\mathcal{F}^{J(\mathrm{pp})}_{[12,34]} \tag{C7}$$

and using Eqs. (C2)–(C4) of Ref. [23] we obtain the following ansatz for this matrix element:

$$\begin{aligned}\mathcal{F}^{J(\mathrm{pp})}_{(12)\eta,\,(34)\eta'} &= \delta_{q_1,\,q_2}\,\delta_{q_3,\,q_4}\,\delta_{q_1,\,q_3}\,\frac{1}{2J+1}\,\langle j_2l_2 ||\, T_{J\,J\,0} \,||\, j_1l_1\rangle \\ &\quad \times \langle\, j_4l_4 ||\, T_{J\,J\,0} \,||\, j_3l_3\rangle\big[\delta_{\eta,\eta'}(u_{(1)}u_{(2)}u_{(3)}u_{(4)} \\ &\quad + v_{(1)}v_{(2)}v_{(3)}v_{(4)}) - \delta_{\eta,-\eta'}(u_{(1)}u_{(2)}v_{(3)}v_{(4)} \\ &\quad + v_{(1)}v_{(2)}u_{(3)}u_{(4)})\big]\int_0^\infty dr\, r^2 R_{(1)}(r)\, R_{(2)}(r) \\ &\quad \times R_{(3)}(r)\, R_{(4)}(r)\mathcal{F}^{\xi}(r). \qquad \text{(C8)}\end{aligned}$$

Note that the value of $\mathcal{F}^{J(\mathrm{pp})}_{(12)\eta,\,(34)\eta'}$ in Eq. (C8) of the present paper differs from the corresponding value derived from

Eqs. (C2) and (C3) of Ref. [23] by a factor of 1/2 owing to the shorthand summation used in Eq. (C1) [(3) $\leqslant$ (4)]. In addition, in the case $J = 0$ one should set $\mathcal{F}^{J(\mathrm{pp})}_{(12)\eta,\,(34)\eta'} = \delta_{(12)}\,\delta_{(34)}\,\mathcal{F}^{J(\mathrm{pp})}_{(11)\eta,\,(33)\eta'}$ to obtain consistency with the gap equation (A25) of Ref. [23] written in the diagonal approximation. Note that this method is applicable both in the QTBA and in the QRPA. In the latter case the amplitudes $\Phi^{J(\mathrm{res})}$ in Eq. (C6) are set to be equal to zero.

[1] D. H. Youngblood, H. L. Clark, and Y.-W. Lui, Phys. Rev. Lett. **82**, 691 (1999).
[2] J. P. Blaizot, D. Gogny, and B. Grammaticos, Nucl. Phys. **A265**, 315 (1976).
[3] O. Bohigas, A. M. Lane, and J. Martorell, Phys. Rep. **51**, 267 (1979).
[4] J. P. Blaizot, Phys. Rep. **64**, 171 (1980).
[5] J. Treiner, H. Krivine, O. Bohigas, and J. Martorell, Nucl. Phys. **A371**, 253 (1981).
[6] J. P. Blaizot, J. F. Berger, J. Dechargé, and M. Girod, Nucl. Phys. **A591**, 435 (1995).
[7] M. Farine, J. M. Pearson, and F. Tondeur, Nucl. Phys. **A615**, 135 (1997).
[8] N. Van Giai, P. F. Bortignon, G. Colò, Z.-M. Ma, and M. R. Quaglia, Nucl. Phys. **A687**, 44c (2001).
[9] S. K. Patra, X. Viñas, M. Centelles, and M. Del Estal, Nucl. Phys. **A703**, 240 (2002).
[10] V. B. Soubbotin, V. I. Tselyaev, and X. Viñas, Phys. Rev. C **69**, 064312 (2004).
[11] G. Colò, N. Van Giai, J. Meyer, K. Bennaceur, and P. Bonche, Phys. Rev. C **70**, 024307 (2004).
[12] H. Sagawa, S. Yoshida, G.-M. Zeng, J.-Z. Gu, and X.-Z. Zhang, Phys. Rev. C **76**, 034327 (2007).
[13] P. Ring and J. Speth, Nucl. Phys. **A235**, 315 (1974).
[14] J. Wambach, V. A. Madsen, G. A. Rinker, and J. Speth, Phys. Rev. Lett. **39**, 1443 (1977).
[15] S. Kamerdzhiev, J. Speth, and G. Tertychny, Phys. Rep. **393**, 1 (2004).
[16] D. Vretenar, T. Nikšić, and P. Ring, Phys. Rev. C **68**, 024310 (2003).
[17] T. Nikšić, D. Vretenar, G. A. Lalazissis, and P. Ring, Phys. Rev. C **77**, 034302 (2008).
[18] T. Li *et al.*, Phys. Rev. Lett. **99**, 162503 (2007).
[19] V. G. Soloviev, *Theory of Atomic Nuclei: Quasiparticles and Phonons* (Institute of Physics, Bristol and Philadelphia, 1992).
[20] P. F. Bortignon and R. A. Broglia, Nucl. Phys. **A371**, 405 (1981).
[21] V. I. Tselyaev, Yad. Fiz. **50**, 1252 (1989) [Sov. J. Nucl. Phys. **50**, 780 (1989)].
[22] V. I. Tselyaev, Phys. Rev. C **75**, 024306 (2007).
[23] E. V. Litvinova and V. I. Tselyaev, Phys. Rev. C **75**, 054318 (2007).
[24] F. Tondeur, M. Brack, M. Farine, and J. M. Pearson, Nucl. Phys. **A420**, 297 (1984).
[25] Y. Aboussir, J. M. Pearson, A. K. Dutta, and F. Tondeur, Nucl. Phys. **A549**, 155 (1992).
[26] S. Krewald, V. B. Soubbotin, V. I. Tselyaev, and X. Viñas, Phys. Rev. C **74**, 064310 (2006).
[27] S. Shlomo and G. Bertsch, Nucl. Phys. **A243**, 507 (1975).
[28] A. P. Platonov and E. E. Saperstein, Nucl. Phys. **A486**, 63 (1988).
[29] A. B. Migdal, *Theory of Finite Fermi Systems and Applications to Atomic Nuclei* (Interscience, New York, 1967).
[30] S. Kamerdzhiev, R. J. Liotta, E. Litvinova, and V. Tselyaev, Phys. Rev. C **58**, 172 (1998).
[31] J. Piekarewicz, Phys. Rev. C **76**, 031301(R) (2007).
[32] D. H. Youngblood, Y.-W. Lui, H. L. Clark, B. John, Y. Tokimoto, and X. Chen, Phys. Rev. C **69**, 034315 (2004).
[33] M. Uchida *et al.*, Phys. Rev. C **69**, 051301(R) (2004).
[34] M. Itoh *et al.*, Phys. Rev. C **68**, 064602 (2003).
[35] A. Avdeenkov, F. Grümmer, S. Kamerdzhiev, S. Krewald, E. Litvinova, N. Lyutorovich, S. Speth, and V. Tselyaev, arXiv: 0808.0478v2 [nucl-th].
[36] T. Sil, S. Shlomo, B. K. Agrawal, and P.-G. Reinhard, Phys. Rev. C **73**, 034316 (2006).
[37] V. I. Tselyaev, Izv. Ross. Akad. Nauk, Ser. Fiz. **64**, 541 (2000) [Bull. Russ. Acad. Sci., Phys. (USA) **64**, 434 (2000)].